

Bonding interface zone of Mg-Gd-Y/Mg-Zn-Gd laminated composite fabricated by equal channel angular extrusion

WU Di(吴迪)^{1,2}, CHEN Rong-shi(陈荣石)¹, HAN En-hou(韩恩厚)¹

1. State Key Laboratory for Corrosion and Protection, Institute of Metal Research, Chinese Academy of Sciences, Shenyang 110016, China;
2. Graduate School of Chinese Academy of Sciences, Beijing 100049, China

Received 23 September 2009; accepted 30 January 2010

Abstract: In order to improve the mechanical properties and corrosion resistance of Mg alloys, the equal channel angular extrusion (ECAE) was employed to fabricate the Mg-5Gd-5Y/Mg-2Zn-1Gd (GW55/ZG21) laminated composites. After fabrication and annealing treatment, the microstructural evolution, phase constitution, microhardness, and bonding strength were investigated on the bonding interface zone of GW55/ZG21 laminated composites. The bonding interface zone of GW55/ZG21 laminated composites comprises a lot of $Mg_3(Y, Gd)_2Zn_3$ particles along the bonding interface, some rod $Mg_{24}(Y, Gd)_5$ phases on GW55 side, and a precipitation free zone (PFZ) on ZG21 side. After annealing treatment, $Mg_3(Y, Gd)_2Zn_3$ particles along the bonding interface increase, rod $Mg_{24}(Y, Gd)_5$ phases on GW55 side decrease, and PFZ is broadened. Meanwhile, the hardness on the bonding interface zone decreases and the bonding strength increases from 126 MPa to 162 MPa.

Key words: magnesium alloys; laminated composite; equal channel angular extrusion; bonding interface; bonding strength

1 Introduction

Magnesium alloys are becoming increasingly attractive for potential use in a wide range of structural applications because of their low density, good machinability, and favorable recycling capability[1–2]. However, their applications are limited due to poor corrosion resistance, low strength or ductility compared with widely used structural materials like steels and Al alloys. As a result, a number of investigations have been focused on the development of Mg-based composites. The Al/Mg-Li alloy clad plate has been fabricated by the cold rolling method and exhibits excellent formability during the 180° bending test after annealing treatment at 150 °C and 200 °C [3]; while accumulative roll bonding could also produce a significant grain refinement and good interface bonding for similar AZ61 alloys and dissimilar Mg-Ni laminated composite[4–5].

In general, the bonding processes mentioned above require special facilities, complex equipment or high-cost instrument, etc. Recently, the equal channel angular extrusion (ECAE) technique, which has been mainly

used to refine the microstructures of bulk materials, was novelly employed to fabricate the laminated composites[6–7]. Dimensional precision and simple bonding process are among the advantages of this method. The Mg-Y-Nd/Mg-Zn-Y laminated composite fabricated by ECAE exhibits high tensile ductility even superplasticity at various temperatures and strain rates[6]. Meanwhile, LIU et al[7] studied the phase constitutions near the interface of Mg-Al-Zn/Al bimetal structure prepared by ECAE. However, for laminated composite between similar metals fabricated by ECAE, microstructural characteristics near the interface have not been researched, and the bonding properties are seldom discussed. In the present work, the laminated composite of Mg-5Gd-5Y/Mg-2Zn-1Gd (GW55/ZG21) was fabricated by ECAE. The microstructural characteristics on bonding interface zone and bonding properties of GW55/ZG21 were observed and analyzed.

2 Experimental

The materials used in the experiments were the rolled ZG21 (Mg-1.47Zn-1.05Gd) (mass fraction, %)

alloy and the extruded GW55 (Mg-4.77Gd-5.04Y-0.53Zr) alloy. The extruded GW55 alloy was isothermally aged at 200 °C for 24 h.

GW55 and ZG21 with a rectangular cross-section of 12 mm×6 mm and a height of 100 mm were machined parallel to the extrusion or rolling direction. Surface treatments on the sand paper with water were applied to the alloys, which could bring about a rugged surface; subsequently, drying treatment was performed immediately. The ECAE die with a square cross-section of 12 mm×12 mm and an intersecting angle of 90° had a horizontal L-shaped configuration as shown in Fig.1. For the cuboid billet, there are four surfaces parallel to extrusion direction. The surface close to the inside corner Φ during extrusion is denoted as top surface, and the opposite one is denoted as bottom surface. Other two surfaces are the side surfaces. The ECAE die was firstly preheated to 350 °C. The assembled GW55 and ZG21 components were placed into the die with the interface between two components perpendicular to the top surface. 5–7 min was needed to equilibrate temperature before ECAE. Subsequently, the synthesizing procedure was carried out with a feeding rate of 2 mm/min. Only one pass ECAE was carried out for fabrication of the laminated composites. After ECAE, the composites were annealed at 350 °C for 1 h to increase the bonding strength.

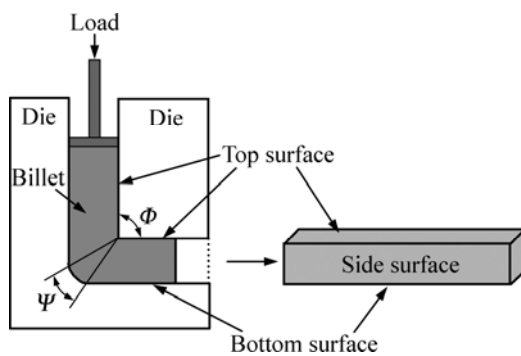


Fig.1 Schematic of ECAE process

The microstructure near the bonding interface on the top surface was observed by means of scanning electron microscope (SEM, Philips XL30 ESEM-FEG/EDAX) equipped with an energy-dispersive X-ray (EDX) spectroscopy analysis system. The metallography specimen was cut along the bonding interface. The phase constitution on each bonding interface was analyzed by Rigaku D/max 2400 X-ray diffractometer with Cu K_{α} target.

The micro Vickers hardness near the bonding interface was measured by means of microscrometer, using a 1.96 N load and a loading time of 10 s.

The bonding strength of GW55/ZG21 laminated composites was measured by tensile test normally to the

bonding interface in the SANS-CMT5105 tensile testing machine. The compact tensile specimens in dog-bone shape with a gauge length of 3.5 mm and a cross-section of 3 mm×2 mm had tensile axes perpendicular to the bonding interface. The interface was kept in the middle of the length.

3 Results

3.1 Macrostructural characteristics

Fig.2 shows the appearances of GW55/ZG21 laminated composites fabricated by ECAE. The bonding of the interface between two materials during ECAE is important for the performance of the laminates[8]. No discernible defects such as cracks or voids at the interface suggest that ECAE technique is very efficient in fabricating laminated composites. The interface lines on top surface along the extrusion direction are not very straight, which is suggested to be attributed to the difference in the flow behavior of the alloys during extrusion[9].

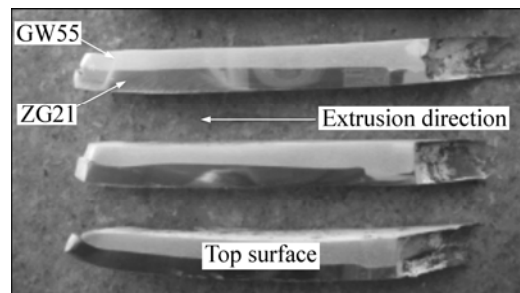


Fig.2 Appearances of GW55/ZG21 laminated composites fabricated by ECAE

3.2 Microstructural characteristics

Fig.3 exhibits the microstructures of the bonding interface zone of GW55/ZG21 laminated composites before and after annealing treatment at 350 °C. The interface presents a jagged profile. For laminated composites between dissimilar metals, there usually appear one or several interfacial diffusion layers distributed along the interface, which consist of intermetallic compounds formed from major elements diffusing from both mating halves, and have a great contrast difference from its neighborhood[6, 10, 11]. In the present study, no interfacial diffusion layer is found, even for the one after annealing treatment. However, there still exist some new phases on the bonding interface zone, which are different from the phases in constituent matrix in morphology or distribution. A lot of new phases with rod morphology can be found on the bonding interface zone close to GW55 side. According to EDX results in Table 1, the rod phases mainly consist of Mg, Gd and Y, and the composition of Mg in the rod phases is around 83%, which indicates that the

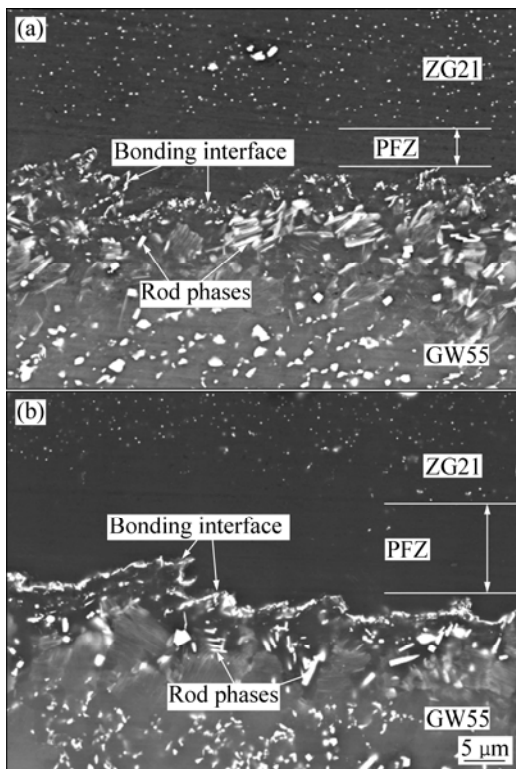


Fig.3 Microstructures of bonding interface zone of GW55/ZG21 laminated composites fabricated at 350 °C (a) and followed by annealing at 350 °C for 1 h (b)

Table 1 Compositions of bonding interface zone of GW55/ZG21 laminated composites in Fig.2 (mole fraction, %)

Element	Before annealing treatment		After annealing treatment	
	Rod phases	Particles along interface	Rod phases	Particles along interface
Mg	82.26	40.06	83.29	38.21
Y	10.25	15.21	11.87	16.83
Gd	7.49	10.50	4.60	8.38
Zn	0	34.23	0.24	36.58

stoichiometry of the rod phases is near $Mg_{24}(Y,Gd)_5$ or $Mg_3(Y,Gd)$. There exists a precipitation free zone (PFZ) on the bonding interface zone close to ZG21 side, where few second phases can be found. Next to the PFZ, a lot of fine particles distribute along the bonding interface. The composition of these particles is determined to be approximately $Mg_3(Y,Gd)_2Zn_3$ by EDS analysis in accordance with Ref.[12]. After annealing treatment at 350 °C for 1 h, as shown in Fig.3(b), the content of rod phases on the bonding interface zone close to GW55 side decreases; on the contrary, the content of fine particles distributed along the bonding interface increases sharply, so that the particles join together and form a line continuously along the bonding interface. Correspondingly, the PFZ on the bonding interface zone

close to ZG21 side is broadened.

To further clarify the phase constitution in the bonding interface zone of GW55/ZG21 laminated composites, the metallography specimen was separated along the bonding interface. The XRD faces in the test are shown in Fig.4(a). The XRD results on phase constituents near the bonding interface on GW55 side and ZG21 side are shown in Fig.4(b). According to the XRD results, there mainly exist $Mg_3(Y, Gd)_2Zn_3$ phase close to ZG21 side, and $Mg_{24}(Y, Gd)_5$ and $Mg_3(Y, Gd)_2Zn_3$ phases close to GW55 side, respectively. In comparison with the EDX results in Table 1, we can confirm that the rod phase is $Mg_{24}(Y, Gd)_5$ and the particle along the bonding interface is $Mg_3(Y, Gd)_2Zn_3$. After the metallography specimen was separated along the bonding interface, $Mg_3(Y, Gd)_2Zn_3$ phases can be found in both sides of the interface, which indicates the $Mg_3(Y, Gd)_2Zn_3$ phases indeed distribute along the bonding interface.

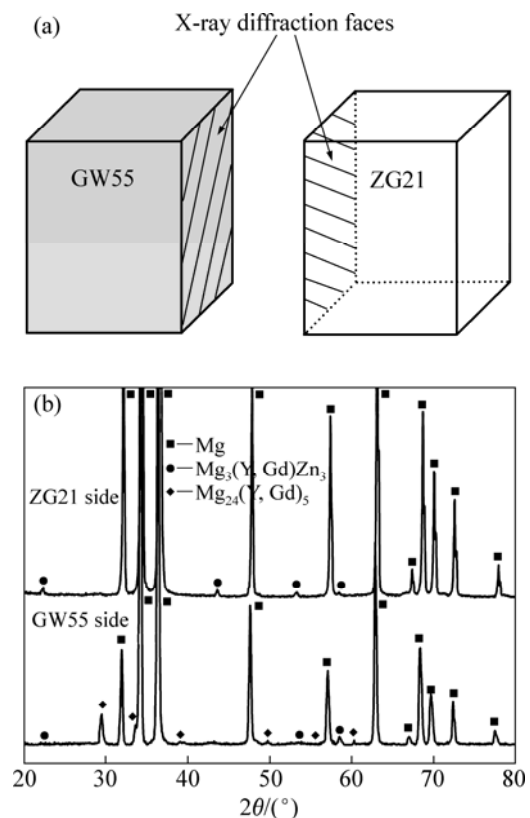


Fig.4 XRD patterns on bonding interface zone of GW55/ZG21 laminated composites fabricated at 350 °C

3.3 Vickers hardness

The micro Vickers hardness near the bonding interface is shown in Fig.5. The starting point is on GW55 side, and positive direction point to ZG21 side and perpendicular to the bonding interface. Before annealing treatment, the microhardness near the bonding interface decreases from GW55 side (about HV80) to

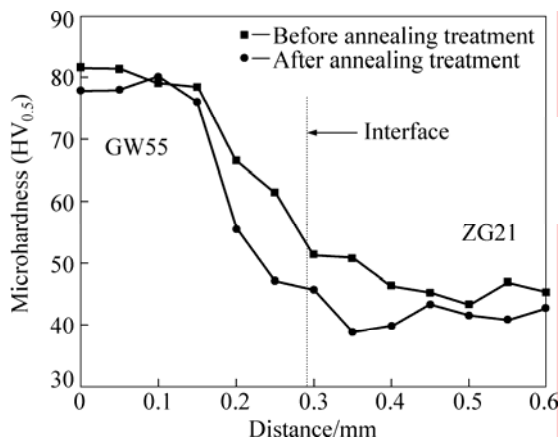


Fig.5 Microhardness near bonding interface

ZG21 side (HV45). There is no peak value appearing near the bonding interface, which is due to no interfacial diffusion layer forming[12]. After annealing treatment, the microhardness on both sides of the interface and the trend of microhardness—distance curve have little change. However, the microhardness in the bonding interface zone (in the range of about 1 mm away from the bonding interface) decreases obviously.

3.4 Bonding strength

Fig.6 shows the results of tensile test normal to the bonding interface. The ultimate tensile strength of GW55/ZG21 laminated composite with the bonding interface parallel to the tensile direction is also included[13]. The results of the tensile test normal to the bonding interface are mainly dependent on the real metallurgical properties of the bonding interface, so ultimate tensile strength (UTS) of the tensile test is defined as the bonding strength of GW55/ZG21 laminated composites. It can be seen that the bonding strength of GW55/ZG21 laminated composites can be up

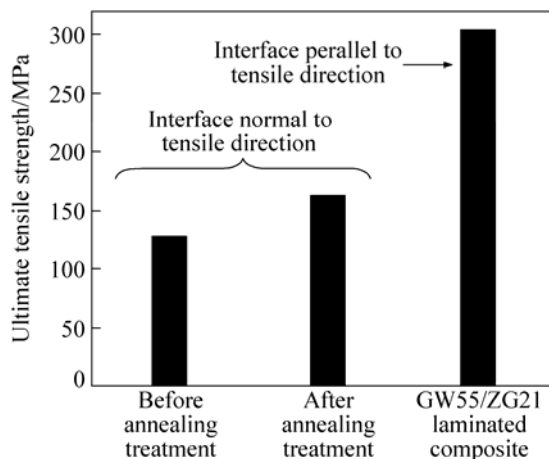


Fig.6 Bonding strength of GW55/ZG21 laminated composites fabricated at 350 and followed by annealing at 350 for 1 h

to 126 MPa, which is approximately 41% of the UTS of GW55/ZG21 laminated composite with the bonding interface parallel to the tensile direction. After annealing treatment, the bonding strength is more satisfactory, and increases to 162 MPa, which is approximately 53% of the UTS of GW55/ZG21 laminated composite with the bonding interface parallel to the tensile direction.

4 Discussion

GW55/ZG21 laminated composites with good bonding quality are fabricated by ECAE. Due to the different flow behaviors of two constituent alloys during extrusion, the bonding interface curves a little in macroscopic view. Such a variation of the bonding interface along extruding direction is in agreement with previously published results in the case of conventional co-extrusion of bimetals[8]. As in the ECAE process a relatively high pressure is applied on the material[14] and also a severe shear deformation is imposed on the material[15], a good interlocking wave structure is generated between the two components in microscopic view, as shown in Fig.3, resulting in a higher bonding strength rather than other bonding process, such as diffusion bonding or general extrusion process[16].

During ECAE bonding process, the elements of Gd, Y and Zn interdiffuse across the bonding interface along the concentration gradient[6]. The chemical attraction appears on the bonding interface and then the new chemical power presents caused by atomic diffusion[17]. Meanwhile, a lattice distortion zone is formed near the bonding interface due to the extrusion and shear deformation between two components during ECAE, where the thermodynamic driving force of precipitation of new phase is high[10, 17]. Therefore, after the concentration of Gd, Y and Zn reaches a certain level, crystal nuclei of the second intermetallic compound, like $Mg_{24}(Y, Gd)_5$ in rod shape and $Mg_3(Y, Gd)_2Zn_3$ particles, are formed on the bonding interface zone and grow up[18]. Since the concentration of Zn must be higher in the bonding interface zone close to ZG21 side, the $Mg_3(Y, Gd)_2Zn_3$ forms along the interface close to ZG21 side. In consideration of the lower content of Gd, Y and Zn on ZG21 side and most of them near the bonding interface diffusing to the interface to form $Mg_3(Y, Gd)_2Zn_3$ particles, the concentration of Gd, Y and Zn on the bonding interface zone close to ZG21 side cannot reach the level to form the second intermetallic compound. So, a PFZ appears in the bonding interface zone close to ZG21 side.

Interfacial diffusion layer, consisting of large amount of intermetallic compounds, forms when bonding between dissimilar materials takes places[19–20]. However, in the present study, two components are both

Mg alloys, Gd, Y and Zn are all not major elements in two components, and the total content of them is lower than 15%, which limits the quantity of the new phases forming in the bonding interface zone, thus there is no interfacial diffusion layer forming. And the hardness drops from GW55 side to ZG21 side across the bonding interface, without peak value appearing. The brittle intermetallic compounds formed could weaken the bonding performance[21]. The lower content of intermetallic compounds near the bonding interface also benefits the bonding strength.

It has been reported that the melting temperature of $Mg_3(Y, Gd)_2Zn_3$ phase is about 510 [22–23], so during annealing treatment at 350 , $Mg_3(Y, Gd)_2Zn_3$ continues forming crystal nuclei and grows up along the bonding interface, resulting in Gd, Y and Zn continue diffusing to the bonding interface. Hence, the PFZ on the bonding interface close to ZG21 side is wider than the one before annealing treatment, and some $Mg_{24}(Y, Gd)_5$ rod phases melt, which is supposed to be the higher nucleation work of $Mg_{24}(Y, Gd)_5$ at 350 . Because $Mg_3(Y, Gd)_2Zn_3$ phase basically has no strengthening effect[24–25] and the changes in the zone beside the bonding interface both generate a softening effect, although the content of $Mg_3(Y, Gd)_2Zn_3$ phases increase along the bonding interface, the microhardness in the bonding interface zone decreases somewhat after annealing treatment. There is no direct proof to support the detrimental effect of $Mg_3(Y, Gd)_2Zn_3$ phase on the mechanical properties of alloys[11]. The annealing treatment can be expected to develop a strong metallurgical bond at the original interface[26], and the bonding strength of GW55/ZG21 laminated composite increases by 36 MPa after annealing treatment.

5 Conclusions

1) Mg based laminated composites of GW55/ZG21 are successfully fabricated by means of ECAE. The bonding interface curves a little in macroscopic view.

2) The bonding interface zone of GW55/ZG21 laminated composites comprises lots of $Mg_3(Y, Gd)_2Zn_3$ particles along the bonding interface, some rod $Mg_{24}(Y, Gd)_5$ phases on GW55 side, and a PFZ on ZG21 side.

3) The hardness drops from GW55 side to ZG21 side across the bonding interface, without peak value appearing. The bonding strength is almost 130 MPa by just one pass ECAE. The excellent bonding strength can be attributed to the strong metallurgical bond, the interlocking wave structure, and the lower content of intermetallic compounds in the bonding interface zone.

4) Annealing treatment causes $Mg_3(Y, Gd)_2Zn_3$ particles along the bonding interface to increase, rod $Mg_{24}(Y, Gd)_5$ phases on GW55 side to decrease, and PFZ

on ZG21 side to be broadened. Meanwhile, the hardness in the bonding interface zone decreases and the bonding strength increases by 36 MPa after annealing treatment.

References

- [1] BUHA J. Natural ageing in magnesium alloys and alloying with Ti [J]. *Journal of Materials Science*, 2008, 43: 1220–1227.
- [2] HUANG X S, SUZUKI K, WATAZU A, SHIGEMATSU I, SAITO N. Microstructure and texture of Mg-Al-Zn alloy processed by differential speed rolling [J]. *Journal of Alloys and Compounds*, 2008, 457: 408–412.
- [3] MATSUMOTO H, WATANABE S, HANADA S. Fabrication of pure Al/Mg-Li alloy clad plate and its mechanical properties [J]. *Journal of Materials Processing Technology*, 2005, 169: 9–15.
- [4] DEL WALLE J A, PEREZ-PRADO M T, RUANO O A. Accumulative roll bonding of a Mg-based AZ61 alloy [J]. *Materials Science and Engineering A*, 2005, 410/411: 353–357.
- [5] UEDA T T. Preparation and hydrogen storage properties of Mg-Ni-Mg₂Ni laminate composites [J]. *Journal of Alloys and Compounds*, 2005, 386: 253–257.
- [6] LIU Xi-bo, CHEN Rong-shi, HAN En-hou. High temperature deformations and microstructural evolutions of Mg alloy laminated composites fabricated by ECAE [C]//NYBERG E A, AGNEW S R, NEELAMEGGHAM N R, MIHRIBAN. *Proceeding of Magnesium Technology Symposium 2009*. San Francisco, USA, 2009: 515–520.
- [7] LIU Xi-bo, CHEN Rong-shi, HAN En-hou. Preliminary investigations on the Mg-Al-Zn/Al laminated composite fabricated by equal channel angular extrusion [J]. *Journal of Materials Processing Technology*, 2009, 209: 4675–4681.
- [8] PAWEL K, MARIO E E, WOJCIECH Z M. Bi-metal rod extrusion—process and product optimization [J]. *Materials Science and Engineering A*, 2004, 369: 170–180.
- [9] GRAVIER S, PUECH S, BLANDIN J J, SUERY M. New metallic glass/alloy (MeGA) rods produced by co-extrusion [J]. *Adv Eng Mate*, 2006, 10: 948–953.
- [10] HE P, LIU D. Mechanism of forming interfacial intermetallic compounds at interface for solid state diffusion bonding of dissimilar materials [J]. *Materials Science and Engineering A*, 2006, 437: 430–435.
- [11] REN Jiang-wei, LI Ya-jiang, FENG Tao. Microstructure characteristics in the interface zone of Ti/Al diffusion bonding [J]. *Materials Letters*, 2002, 56: 647–652.
- [12] XU D K, TANG W N, LIU L, XU Y B, HAN E H. Effect of W-phase on the mechanical properties of as-cast Mg-Zn-Y-Zr alloys [J]. *Journal of Alloys and Compounds*, 2008, 461: 248–252.
- [13] WU Di, CHEN Rong-shi, HAN En-hou. Microstructural and mechanical properties of Mg based laminated composites fabricated by ECAE [C]//KAINER K U. *Proceeding of the 8th International Conference on Magnesium Alloys and their Application*. Weimar, Germany, 2009: 689–695.
- [14] BOWEN J R, GHOLINIA A, ROBERTS S M, PRANGNELL P B. Analysis of the billet deformation behaviour in equal channel angular extrusion [J]. *Materials Science and Engineering A*, 2000, 287: 87–99.
- [15] SEGAL V M. Materials processing by simple shear [J]. *Materials Science and Engineering A*, 1995, 197: 157–164.
- [16] EIVANI A R, TAHERI A K. A new method for producing bimetallic rods [J]. *Materials Letters*, 2007, 61: 4110–4113.
- [17] LI Yun-tao, DU Ze-yu, MA Cheng-yong. Interfacial energy and match of cold pressure welded Ag/Ni and Al/Cu [J]. *Trans Nonferrous Met Soc China*, 2002, 12(5): 814–817.
- [18] XIA Li-fang. Diffusion in metal [M]. Harbin: Harbin Institute of

- Technology Press, 1989. (in Chinese)
- [19] KUNDU S, GHOSH M, LAIK A, BHANUMURTHY K, KALE G B, CHATTERJEE S. Diffusion bonding of commercially pure titanium to 304 stainless steel using copper interlayer [J]. *Materials Science and Engineering A*, 2005, 407: 154–160.
- [20] GHOSH M, DAS S, BANARJEE P S, CHATTERJEE S. Variation in the reaction zone and its effects on the strength of diffusion bonded titanium–stainless steel couple [J]. *Materials Science and Engineering A*, 2005, 390: 217–226.
- [21] ABBASI M, TAHERI A K, SALEHI M T. Growth rate of intermetallic compounds in Al/Cu bimetal produced by cold roll welding process [J]. *Journal of Alloys and Compounds*, 2001, 319: 233–241.
- [22] ZENG X Q, ZHANG Y, LU C, DING W, WANG Y, ZHU Y. Precipitation behavior and mechanical properties of a Mg-Zn-Y-Zr alloy processed by thermo-mechanical treatment [J]. *Journal of Alloys and Compounds*, 2005, 395: 213–219.
- [23] ZHANG Y, ZENG X, LIU L, LU C, ZHOU H, LI Q, ZHU Y. Effects of yttrium on microstructure and mechanical properties of hot-extruded Mg-Zn-Y-Zr alloys [J]. *Materials Science and Engineering A*, 2004, 373: 320–327.
- [24] XU D K, LIU L, XU Y B, HAN E H. Effect of microstructure and texture on the mechanical properties of the as-extruded Mg-Zn-Y-Zr alloys [J]. *Materials Science and Engineering A*, 2007, 443: 248–256.
- [25] XU D K, TANG W N, LIU L, XU Y B, HAN E H. Effect of Y concentration on the microstructure and mechanical properties of as-cast Mg-Zn-Y-Zr alloys [J]. *Journal of Alloys and Compounds*, 2007, 432: 129–134.
- [26] ZHANG L, MENG L, ZHOU S P, YANG F T. Behaviors of the interface and matrix for the Ag/Cu bimetallic laminates prepared by roll bonding and diffusion annealing [J]. *Materials Science and Engineering A*, 2004, 371: 65–71.

(Edited by YUAN Sai-qian)